Electronic Supplementary Material (ESI) for Soft Matter.

Double Stimuli-Responsive Polysaccharide Block Copolymers as *Green* Macrosurfactant for Near-Infrared Photodynamic Therapy

Benjamin B. Breitenbach[a], Elena Steiert[a], Matthias Konhäuser[a], Lea-Marie Vogt[a], Yujen Wang[b], Sapun H. Parekh[b,c], Peter R. Wich[a,d e]*

[a]Institut für Pharmazie und Biochemie, Johannes Gutenberg-Universität Mainz, Staudingerweg 5, 55128 Mainz, Germany

[b]Max Planck Institute for Polymer Research, Ackermannweg 10, 55128 Mainz, Germany

[c]Department of Biomedical Engineering, University of Texas at Austin, Austin, TX, USA

[d]Australian Centre for NanoMedicine, University of New South Wales, Sydney, NSW 2052, Australia

[e]School of Chemical Engineering, University of New South Wales, Sydney, NSW 2052, Australia

phone: +61 2 9385 4308

email: p.wich@unsw.edu.au

web: www.wichlab.com

1) Additional Dex-SH Characterization

The reductive amination reaction with 4-ATP was monitored with ^1H NMR and DOSY NMR. The spectrum shows a single translational diffusion constant for the aromatic protons of the aniline residue (a, a', b, b') and the sugar backbone (AGU) at $9.09 \cdot 10^{-7}$ m^2 s^{-1} (Figure S-1). Reduction of the endgroup modified Dex-SH (**1**) with TCEP or DTT was observed in UV-spectra (A) and ^1H NMR (B) before and after the reduction step (Figure S-2).

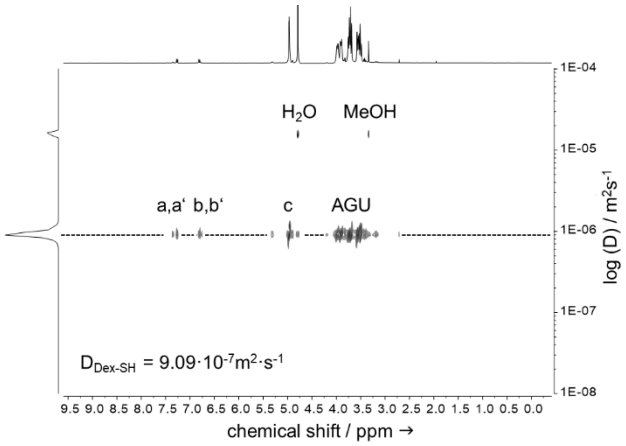

Figure S-1. DOSY ^1H NMR spectra of Dex-SH (**1**) after the reduction with DTT in D_2O (400 MHz). The aromatic protons of the introduced aniline derivative show a single diffusion coefficient. Therefore, it can be concluded, that the reductive amination reaction was successful and work-up sufficient to isolate pure compound (**1**).

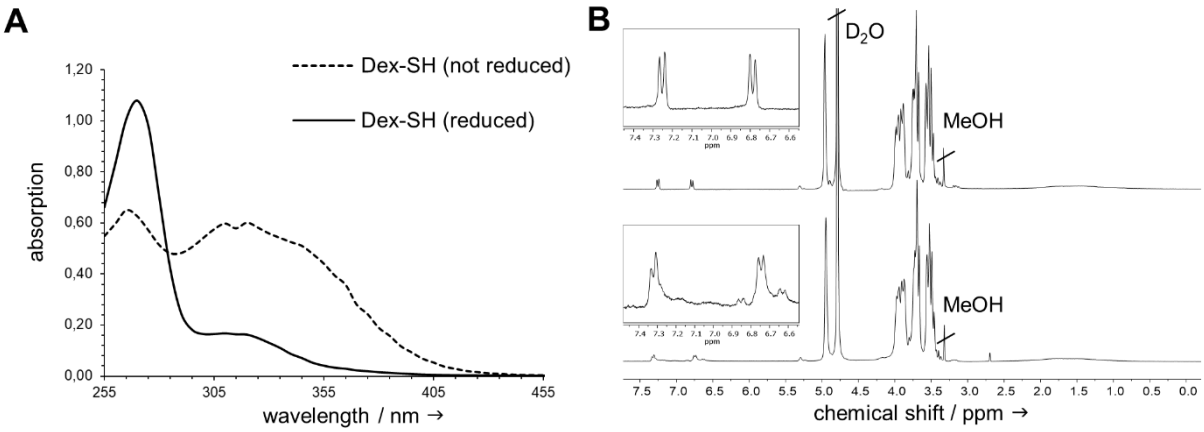

Figure S-2. The reduction of the free thiol group was monitored with UV spectra analysis before (dotted line) and after reduction (straight line) (A). Also ^1H NMR of Dex-SH **1** before (lower spectrum) and after (higher spectrum) treatment with DTT shows a distinct change in the proton signal from broad multiplet signals to two sharp multiplets (B).

The activation of the thiol group on Dex-SH (**2**) was monitored by ^1H NMR and *Raman* spectroscopy. To ensure the S–H stretching mode in Dex-SH was correctly assigned, a *Raman* spectrum of 4-ATP was measured (Figure S-3).

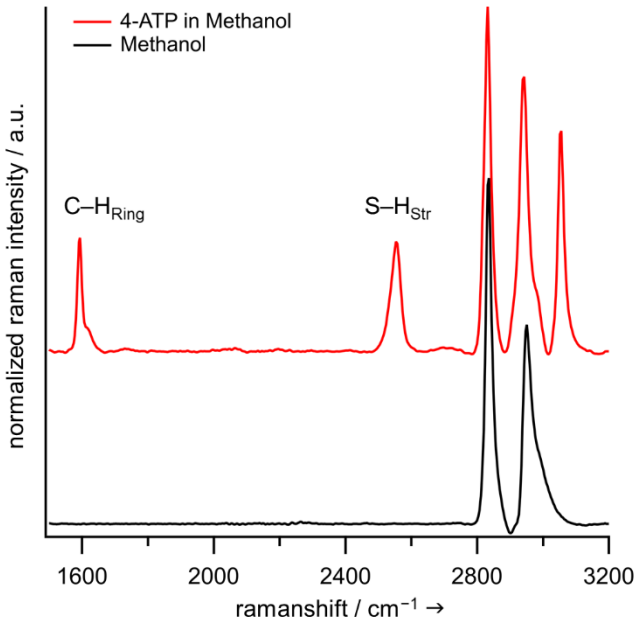

Figure S-3. The methanol solvent spectrum shows peak positions in the CH-region: 2943 cm^{-1} as CH_3 stretching and 2834 cm^{-1} as CH_3 stretching.[1] In contrast, 4-aminothiophenol (4-ATP) dissolved in methanol shows four distinctive peaks: 3056 cm^{-1} the benzene CH stretching, 2951 cm^{-1} as CH_3 stretching, and 1604 cm^{-1} as ring breathing. Here the CH_3 stretching mode was slightly shifted compared to methanol alone.[1] The 4-ATP spectrum also showed a prominent S–H vibration at 2551 cm^{-1}, which is expected for sulfhydryl groups.[2]

2) Additional Dex-S-S-AcDex Characterization

The average g mol^{-1} and the molecular weight of AcDex-S-S-Py (**3**) was calculated by ^1H NMR using equation S-1 (AGU stands for anhydrous glucose unit):

$$\text{n AGU} \cdot \Big(202.22\ (\text{g mol}^{-1}) \cdot \frac{\%}{100}\text{cyclic acetals} + 234.26(\text{g mol}^{-1}) \cdot \frac{\%}{100}\text{acyclic acetals} + 162.12(\text{g mol}^{-1}) \cdot \frac{\%}{100}\text{no acetals}\Big)\,\text{g mol}^{-1} = \text{M}_{\text{n,NMR}}(\text{g mol}^{-1}) \quad \text{(eq. S-1)}$$

Table S-1. Acetal content and theoretical mol. weight of hydrophobic block AcDex-S-S-Py (**3**) and block copolymer Dex-S-S-AcDex (**4**) determined by ^1H NMR. The AcDex-S-S-Py was measured in DMF against PEO standard. Dex-S-S-AcDex was measured in H_2O (0.1 M $NaNO_3$) against a dextran standard.

	total acetal (%)	**cyclic (%)**	**acyclic (%)**	**M_{wNMR} (g mol^{-1})[1]**	**M_{wGPC} (g mol^{-1})[2]**
AcDex-S-S-Py	77.6	45.9	31.7	6102.09	6601.48
Dex-S-S-AcDex	25.6	18	7.6	10246.81	

[1]calculated from ^1H NMR. [2]calculated from GPC

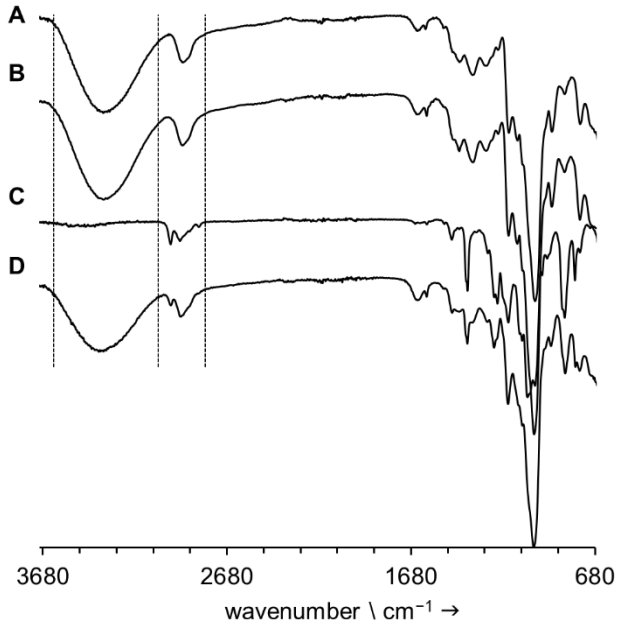

Figure S-4. FTIR spectra of Dex-SH (**A**), Dex-S-S-Py (**B**), AcDex-S-S-Py (**C**) and Dex-S-S-AcDex (**D**). Marked are the O–H vibrational stretch and the C–H vibrational stretch signals.

3) Additional Nanoparticle Characterization

Aggregation Number. Assuming, that the micelle is a hard sphere, the amount of block copolymer chains forming the micellar nanoparticle (aggregation number, N_{ag}) can be estimated from the size of the nanoparticle. The N_{ag} was calculated with equation S-2, like previously reported.[3-6]

$$N_{ag} = \frac{M}{M_0} \qquad \text{(eq. S-2)}$$

Where M is the molecular weight of the micelle (by ^1H NMR) and M_0 the molecular weight of the polymer. A direct determination of the molecular weight of a micelle is possible, however difficult to accomplish. M_0 can be approximated with equation S-3[7]

$$M_0 = \frac{10\pi N_A R^3}{3\upsilon_2} \qquad \text{(eq. S-3)}$$

With R is the radius of the micelle, N_A is Avogadro's number, and υ_2 is the partial specific volume, reported to be approx. 0.611 for dextran.[8-9] R_H of approx. 53.2 nm from DLS.

TEM Measurements of PCZn-loaded Micellar Nanoparticles.

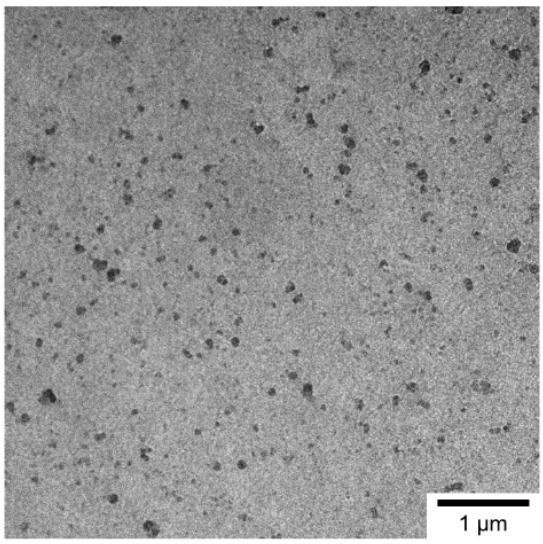

Figure 5. Representative TEM image as overview on drug-loaded Dex-S-S-AcDex nanoparticles. Samples were placed on carbon-coated copper grid (1 mg mL^{-1}) and air-dried before measurement.

Drug Loading and Loading Efficiency. Determination of cargo loading of Dex-S-S-AcDex nanoparticles was carried out with a fluorescence assay (ex: 610 nm; em: 690 nm). Briefly, 0.9 mg lyophilized micelles were dissolved in 700 μL DMSO and triplets of 100 μL were added on a 96 well plate together with an external standard of PC(Zn) in DMSO from $3.08 \cdot 10^{-5}$ mol L^{-1} to $2.41 \cdot 10^{-7}$ mol L^{-1}. Comparing the fluorescence intensity at 690 nm allowed the determination of n(PC(Zn)) in micelles. By varying the initial ratio of mol_{cargo} to $mol_{polymer}$ during particle formation and also the feed (wt%) of cargo to the expected mass of polymer we could change the total amount of encapsulated cargo. The feed of cargo was therefore calculated according to an expected yield of 75% polymer (mol). The $mol_{cargo}/mol_{polymer}$ ratio was calculated with the isolated yield of block copolymer (mg) after the self-assembly and the determined amount of cargo in the whole sample.

The encapsulation efficiency (EE) and the loading content (LC) in weight percentage were calculated with equations S-4 and S-5. The EE was calculated as an encapsulation efficiency of 65.5–84.8%. The loading content resulted in 0.53–2.46% (table S-3). The mass of Dex-S-S-AcDex material was calculated from the lyophilized samples in mg after subtraction of the PC(Zn) content.

$$\text{EE (mol \%)} = \frac{n_{PCZn,encapsulated}}{n_{PCZn,feed}} \cdot 100\% \qquad \text{(eq. S-4)}$$

$$\text{LC (wt. \%)} = \frac{m_{PCZn,encapsulated}}{m_{PCZn,encapsulated} + m_{Polymer}} \cdot 100\% \qquad \text{(eq. S-5)}$$

Table S-2. Optimization of PC(Zn) loading into Dex-S-S-AcDex micellar nanoparticles. The EE and LC were calculated with eq. S-4 and eq. S-5. The mol PC(Zn) was determined by a fluorescence-based assay in DMSO against a PC(Zn) standard (ex. 610 nm, em. 690 nm). The $m_{Polymer}$ was calculated from the isolated nanoparticles and $m_{PC(Zn)}$.

feed (wt%)	$mol_{cargo}/mol_{polymer}$	EE (mol%)	LC (mol%)
0.76	0.09	65.56	0.53
1.76	0.15	66.06	0.85
2.20	0.28	82.45	1.58
3.30	0.45	84.81	2.46

Size and Degradation Measurements by DLS

Table S-3. Characterization of self-assembled, loaded Dex-S-S-AcDex nanoparticles (1.76 wt%), observed over 24 h in aqueous 10 mM NaCl or DMEM-buffer after resuspension of lyophilized samples. The concentration was 10 mg mL^{-1}. Intensity describes the particle size distribution within the sample, depending on their scattering intensities; number represents the size of the particles forming the largest population in the sample.

	initial size			after 24 h		
medium	PdI	intensity (d.nm)	number (d.nm)	PdI	intensity (d.nm)	number (d.nm)
DMEM	0.151	142.9 ± 1.99	70.48 ± 5.76	0.155	153.00 ± 5.23	77.76 ± 4.42
NaCl (10 mM)	0. 160	140.63 ± 3.59	69.88 ± 1.67	0.155	167.86 ± 23.72	76.83 ± 2.92

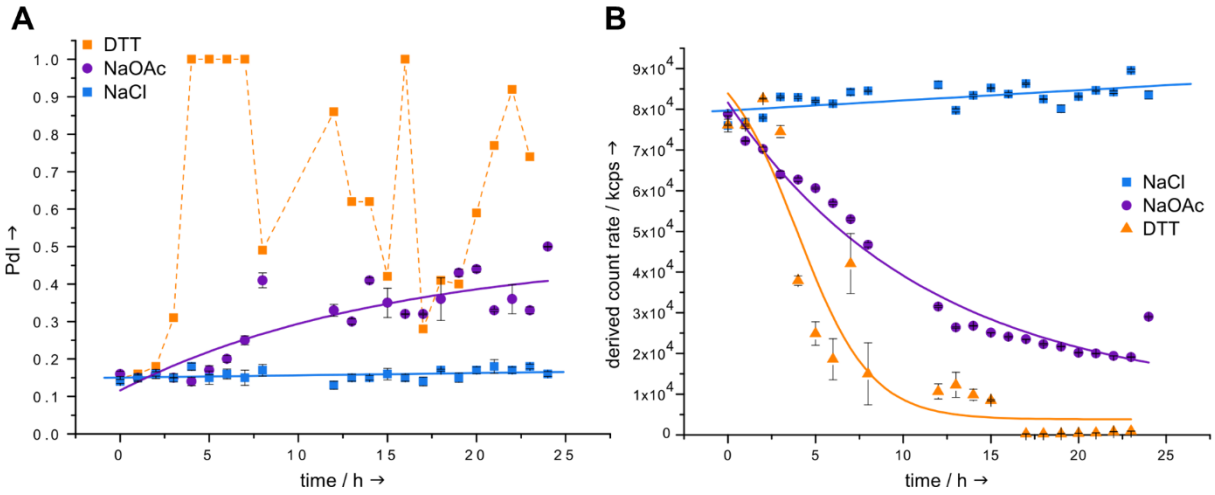

Figure S-6. PdI Values for loaded particles incubated in DTT buffer, NaOAc-buffer and NaCl/H_2O-d. The particles incubated in DTT solution become very polydisperse after 3 h, the largest population precipitates and the PdI decreases again. The residual particles form larger aggregates again, and so on. Particles incubated in NaOAc-buffer become more polydisperse as the material degrades over time and the loaded cargo forms aggregates with residual hydrophobic blocks. Particles incubated at neutral pH keep their monodisperse character (**A**). The derived count rate for particles in neutral pH stays constant indicating no change in concentration of the particle solution. Particles incubated in NOAc-buffer degrade into water soluble material, particles in DTT solution precipitate out of solution. Both effects decrease the number of particles able to scatter the light onto the Zetasizer sensor and therefore decrease the derived count rate (**B**).

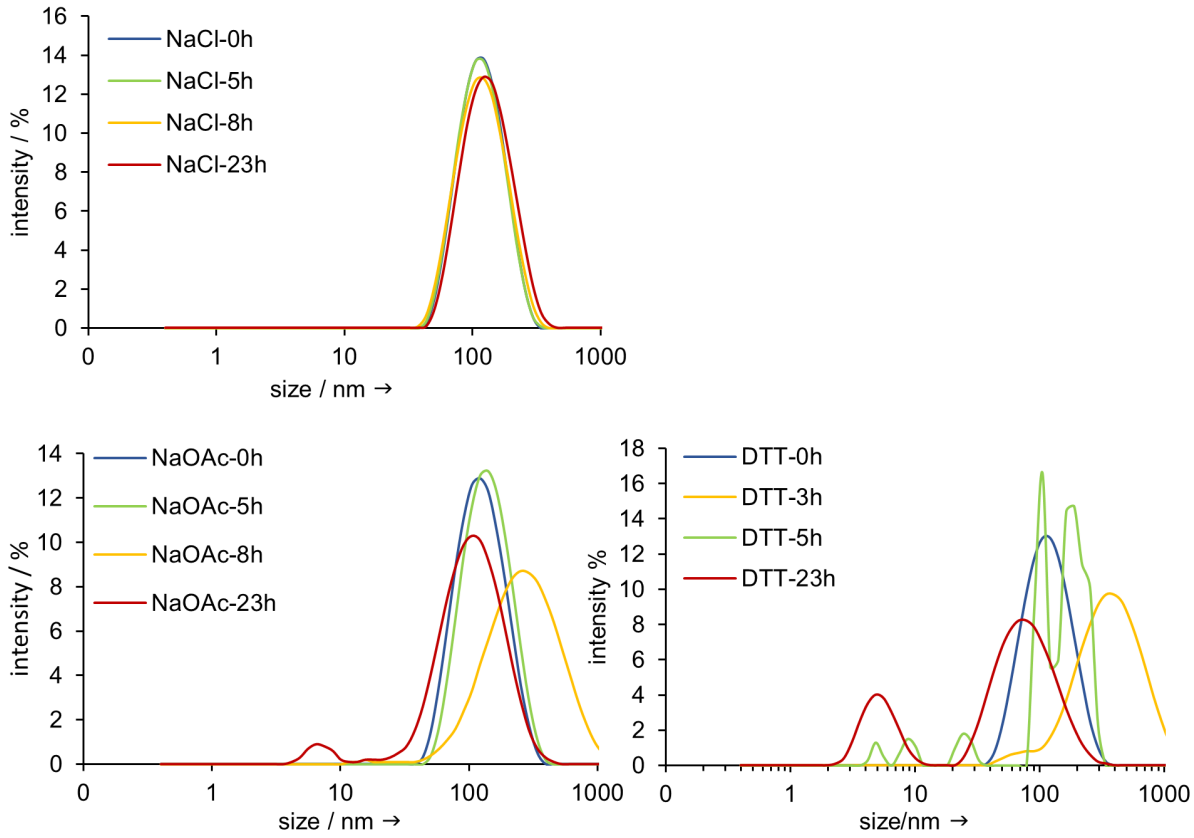

Figure S-7. Size distribution by intensity for loaded particles incubated in neutral buffer (10 mM NaCl), acidic buffer (50 mM NaOAc) or reductive buffer (10 mM DTT/NaCl).

Acknowledgements

We thank *Sandra Seywald* and *Christine Rosenauer* of the MPI-P, Mainz, Germany for the SEC measurements and help with the SLS/DLS light scattering calculations.

Also, we thank *Dr. Frank Depoix* from the Institute of Zoologie of the Johannes Gutenberg-University, Mainz, Germany for the help with TEM measurement preparation and *Stefanie Bürger* from the IMB, Mainz, Germany for the help with flow cytometry data analysis.

Additionally, we thank *Prof. Dr. H. Frey, Prof. Dr. P. Langguth, Prof. Dr. T. Schirmeister and Prof. Dr. T. Effert* (JGU Mainz, Germany) for the kind permission to use some of their analytical equipment.

References

(1) Shimanouchi, T. Tables of Molecular Vibrational Frequencies. *National Bureau of Standards* **1972,** *1*, 1–160.
(2) Bazylewski, P.; Divigalpitiya, R.; Fanchini, G. In situ Raman spectroscopy distinguishes between reversible and irreversible thiol modifications in L-cysteine. *RSC Adv*. **2017,** *7*, 2964–2970.
(3) Schillen, K.; Brown, W.; Johnsen, R. M. Micellar Sphere-to-Rod Transition in an Aqueous Triblock Copolymer System - a Dynamic Light-Scattering Study of Translational and Rotational Diffusion. *Macromolecules* **1994,** *27*, 4825–4832.
(4) Gau, F.; Lacelle, S. 1H NMR Relaxation Studies of the Micellization of a Poly(ethylene oxide)–Poly(propylene oxide)–Poly(ethylene oxide) Triblock Copolymer in Aqueous Solution. *Macromolecules* **1996,** *29*, 170–178.
(5) Jeong, B.; Kibbey, M. R.; Birnbaum, J. C.; Won, Y.-Y.; Gutowska, A. Thermogelling Biodegradable Polymers with Hydrophilic Backbones: PEG-g-PLGA. *Macromolecules* **2000,** *33*, 8317–8322.
(6) Shi, M.; Wosnick, J. H.; Ho, K.; Keating, A.; Shoichet, M. S. Immuno-polymeric nanoparticles by Diels-Alder chemistry. *Angew. Chem. Int. Ed*. **2007,** *46*, 6126–6131.
(7) Owen, S. C.; Chan, D. P. Y.; Shoichet, M. S. Polymeric micelle stability. *Nano Today* **2012,** *7*, 53–65.
(8) Granath, K. A. Solution Properties of Branched Dextrans. *Journal of Colloid Science* **1958,** *13*, 308–328.
(9) Laurent, T. C.; Killander, J. A theory of gel filtration and its exeperimental verification. *Journal of Chromatography A* **1964,** *14*, 317–330.